IEEE Access
Multidisciplinary | Rapid Review | Open Access Journal

Received April 29, 2020, accepted June 14, 2020, date of publication June 26, 2020, date of current version July 20, 2020.

Digital Object Identifier 10.1109/ACCESS.2020.3005239

Closed-Loop Gate Drive for Single-Ended Forward Converter to Reduce Conducted EMI

CONGWEN XU, QISHUANG MA, PING XU, AND NAN WANG
School of Automation Science and Electrical Engineering, Beihang University, Beijing 100191, China
Corresponding author: Qishuang Ma (qsma304@126.com)

ABSTRACT Forward DC/DC converters are widely used in low and medium power circuits that are widely used in the aerospace and navigation fields. Power converters are usually sources of electromagnetic interference (EMI), which is due to their higher voltage and current transients. The traditional method is to add expensive filters on the primary side or the secondary side, but its disadvantages are high cost and poor adjustability. Based on the principle that the greater the number of derivations of voltage transients, the lower the high frequency electromagnetic interference contained in this voltage, a signal containing small high-frequency noise that is suitable for the hardware circuit as a reference signal is selected, and a closed-loop gate drive method is used in this paper, which attenuate the conducted EMI noise in the input bus of the forward DC/DC converter. The reference signal shapes the output signal to achieve the purpose of suppressing electromagnetic interference through the closed loop circuit. The advantages of this method are making the output highly adjustable, reducing hardware size and weight and lower cost compared with filter method. Compared with the method of controlling current to reduce electromagnetic interference, the proposed method is easier to implement. Firstly, the relationship between the derivative order of voltage transient and electromagnetic interference is introduced. Secondly, the experimental principle of single-ended forward circuit controlled by closed loop is introduced. Simulation and experimental results show that the proposed method can achieve voltage shaping and suppression of voltage overshoot effectively. Compared with the traditional hard-switching control method, the proposed method can make the high-frequency components of the drain-source voltage of the primary-side MOS transistor and the secondary-side output voltage have a greater attenuation.

INDEX TERMS Single-ended forward converter, electromagnetic interference (EMI), closed-loop gate derive, reference signal, SiC metal-oxide-semiconductor field-effect transistor (MOSFET).

I. INTRODUCTION

Single-ended forward converter is a common and popular power converter topology. It is widely used in consuming power supplies at 100–300 W power range because of its simple structure and less power electronic components, and its large current output capability and multiple outputs [1]. By analyzing the linear small signal transfer function, singularities can be avoided on the right side of the coordinate axis, which simplify the control method and ensure stable operation of the system [2].

However, at higher power and higher frequency, the phenomenon of electromagnetic interference will be more obvious [3]. EMI noise from high frequencies that results in greater di /dt and dv/dt will interfere with the normal operation of the power converter and cause abnormal operation of the surrounding sensitive components or even damage to them[4] [5]. The electromagnetic interference generated by the single-ended forward power converter must meet one or more international or domestic electromagnetic compatibility standards, such as FCC (Federal Communications Commission), CISPR (International Special Committee on Radio Interference) [6] and EN [7]. A separation network can be used to separate common mode electromagnetic interference and differential mode electromagnetic interference and the detailed method is introduced in [8]. Clamp method [9], [10], [12], EMI filtering technology [4], [11], buffer technology [2], [13],

The associate editor coordinating the review of this manuscript and approving it for publication was Zhuang Xu.

balance technology [14], Soft switching technology [15], [16], [22] and active voltage control method [18]–[20] have been studied by scientists.

A simple RCD clamping circuit, which includes resistors, capacitors, and diodes, is used in forward power converters to provide a release path for the energy in the drain inductance and absorb energy in the magnetizing inductance [9]. However, due to the application of the resistance element R, the energy flowing through R will be lost, so that this method will reduce the efficiency. The combination of active clamping and soft switching technology can effectively reduce EMI, reduce the voltage stress on the MOSFET and improve efficiency [10], [12].

In the reference [4], the hybrid filter method that is a method of combining input active and passive filters to achieve conduction electromagnetic interference noise attenuation is used. The filter is placed on the input end of the DC / DC converter, which can attenuate electromagnetic interference noise without affecting the stability of the converter. Reference [11] used another hybrid method, which is a combination of symmetric topology and passive filtering. Symmetrical topology is well-known for suppressing common-mode electromagnetic interference, but the effect of this method is not obvious in certain frequency bands. The balancing method is to modify the original structure of the converter to obtain a symmetrical circuit structure. The same EMI will be generated in each symmetrical structure, and they cancel each other, so the electromagnetic interference noise contained in the output signal will become very small or disappear. The multi-path hybrid balancing method is used in a dual-switch power converter [14], which includes a power balancing circuit, a transmission line balancing circuit, and a terminal balancing circuit. In this way, the same common mode noise and current are obtained. In reference [21], Symmetrical components are used to reduce the drain-to-source voltage turn-on noise.

Soft-switching converters with coupled inductors are used in [22]. However, under certain conditions, merely reducing the electromagnetic interference through soft switching may not meet the EMI standards. In reference [15], the auxiliary winding and capacitor are added to the soft-switching High Stepdown Converter to achieve better EMI suppression.

Scholar Patrick R. Palmer has studied active voltage control and used it to precisely control the voltage transient of the switch, which is very effective for controlling the electromagnetic interference caused by high dv/dt [18]. In the time domain, the higher the derivative order n of the transient function, the lower the spectral envelope and the smaller the high-frequency electromagnetic interference component [17]. Based on this principle, the literature [19] proposes to use Gaussian functions as the switching Reference signal to achieve the shape of the switching transient to suppress high-frequency electromagnetic interference. The Reference [20] improved the method of using the Gaussian function as a reference signal.

In this paper, considering that high dv/dt will produce high electromagnetic interference, a closed loop is added to the single-ended forward power conversion ventilation circuit, referring to the active voltage control method and the characteristics of the single-ended forward power converter, appropriate Gaussian reference signal is set to control the transient voltage of the switch to improve the conductivity of the transient voltage of the switching MOSFET to reduce the high frequency EMI noise. Moreover, the third winding of the traditional single-ended forward power converter is reserved for magnetic core reset to prevent the establishment of magnetizing current and saturation of the transformer. In Section 2, a closed-loop single-ended forward power converter is proposed. The working principle of the single-ended forward power converter is discussed, including the principle of electromagnetic interference suppression and the output principle of the forward converter in Section 3. The simulation and experimental results are discussed in Section 4. The conclusion based on the experiment is provided in Section 5.

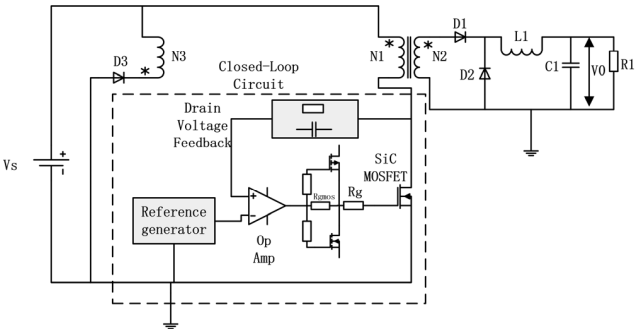

FIGURE 1. The proposed closed-loop single-ended converter.

II. THE TOPOLOGY OF THE PROPOSED SINGLE-ENDED FORWARD CONVERTER

The structure of the proposed closed-loop single-ended forward power converter is shown in FIGURE 1. The closed-loop circuit part and the non-closed-loop circuit part constitute the proposed converter. In the non-closed-Loop circuit, Vs is the input DC voltage source, and N1, N2, and N3 are the primary winding, secondary winding, and demagnetizing winding of the single-item three-winding transformer separately. As the third winding, N3 recovers the energy of the magnetizing inductance to the power supply and resets the transformer core to prevent the generation of magnetic induction current and transformer saturation. The reset of the transformer core requires the cooperation of the reset diode D3. In the secondary side, D1 is a rectifier diode, D2 is a freewheeling diode, and L1 and C1 form an output filter. In the closed-loop circuit, the SiC MOSFET is connected to the primary winding of the transformer, and the source is grounded. The drain voltage is fed back to the operational amplifier through the drain voltage feedback circuit and compared with the reference signal generated by the reference signal generator. Then, the comparison result is amplified

by the drive circuit to control the turn-on turn-off voltage transient of the SiC MOSFET.

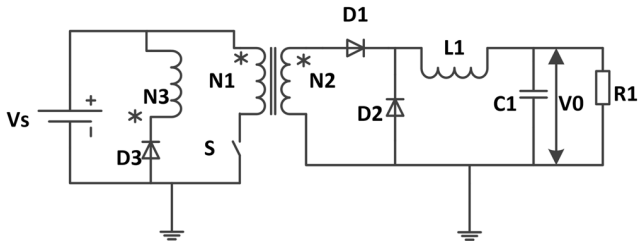

FIGURE 2. The equivalent circuit of the non-closed loop circuit.

III. THE CIRCUIT PARAMETER DESIGN

A. PARAMETER DESIGN AND PRINCIPLE OF NON-CLOSED LOOP CIRCUIT

The equivalent circuit of the non-closed loop circuit, the circuit outside the dashed rectangular frame, is shown in FIGURE 2. In this paper, the input voltage Vs is set to 100V, the output voltage V0 is set to 25V, the output voltage ripple does not exceed 5%, the rated load resistance R1 is 25Ω, the switching frequency f_s is positioned at 200 kHz, and the duty cycle D is 0.5. According to these calculations, the LC output the required inductance and capacitance of the filter and the turns ratio of the three windings of the transformer.

According to reference [23], the forward converter transformation ratio formula is:

$$\mathrm{M} = \frac{V_0}{V_s} = \frac{N_2}{N_1}\mathrm{D} \tag{1}$$

In Equation (1), N2 is the number of turns of the secondary winding of the transformer, and N1 is the number of turns of the primary winding of the transformer, D is the duty cycle. Take the set parameters into the above formula to get N1/N2 = 0.5.

The topology of the single-ended forward converter determines that its isolation transformer needs a magnetic flux reset winding N3 to release the magnetic energy stored in the primary winding N1. Assuming that the working period of the MOS tube is $\mathrm{T_s}$, the on-time of the MOSFET is $\mathrm{T_{on}} = \mathrm{DT_s}$. When the MOSFET is on, the magnetic flux increase on the transformer core is expressed as:

$$\Delta\Phi = (V_S/N_1)\mathrm{T_{on}} = (V_S/N_1)\mathrm{DT}_s \tag{2}$$

When the MOSFET is in the $T_{off} = (1-D)T_s$ off period, S is blocked so that the power supply stops supplying power to the primary winding, and the magnetic flux in the transformer core is reduced, then the magnetic flux reset coil returns the magnetic energy stored in the power transformer to the power supply. If the current in the flux reset coil of the MOS tube is not attenuated to zero during the entire off period, when diode D3 is suppressed to a point during the entire off period, the maximum value of the reduction of the magnetic flux is:

$$\Delta\Phi' = Vs \cdot T_{off}/N_3 = V_S(1-D)T_s/N_3 \tag{3}$$

During the $\mathrm{T_{on}}$ period, the increment $\Delta\Phi$ of the magnetic flux Φ is proportional to the duty cycle D. If the increment $\Delta\Phi$ of the magnetic flux Φ during the $\mathrm{T_{on}}$ period is greater than the maximum decrease $\Delta\Phi'$ during the $\mathrm{T_{off}}$ period, assuming $\Delta\Phi > \Delta\Phi'$, the following equation can be obtained:

$$D > N_1/(N_1+N_3) = D_{\max} \tag{4}$$

If $D > N_1/(N_1+N_3) = D_{max}$, then $\Delta\Phi > \Delta\Phi'$. At the end of each cycle, the magnetic flux of the core will increase by $\Delta\Phi - \Delta\Phi'$, then the core will quickly enter the saturation working area, resulting in the transformer not working properly and the power converter failing. If $D < N_1/(N_1+N_3) = D_{max}$, the magnetic flux in the secondary winding has decayed to zero before the SiC MOSFET turn-off time is over in one cycle, so that the converter can work normally. $D_{max} = N_1/(N_1+N_3)$ is the maximum duty cycle allowed, and $D \le D_{max}$ must be guaranteed in the actual project. In this paper, it is assumed that $\mathrm{N_3} = \mathrm{N_1}$, so the maximum duty cycle is 0.5, N1:N2:N3 = 2:1:2.

According to reference [23], in order to ensure that the filter inductor current is continuous under rated load, the following conditions must be met:

$$L \ge \frac{V_0}{2f_sI}(1-D) \tag{5}$$

Duty ratio D 0.5, current I 1A, output voltage V0 25V, switching frequency fs 200 kHz, are taken into the formula to get $L \ge 31.25\ \mu H$. Considering that the nominal and actual values of the actual inductance leave a certain margin, the 220 μH filter inductance is selected. The calculation formula of output voltage ripple is:

$$\frac{\Delta V0}{V0} = \frac{1-D}{8LCf_s^2} = \frac{\pi^2}{2}(\frac{f_c}{f_s})^2(1-D) \tag{6}$$

where $\mathrm{f_c}$ is the cutoff frequency of the LC filter, and its expression is:

$$f_c = \frac{1}{2\pi\sqrt{LC}} \tag{7}$$

Take the 220uF filter capacitor and filter inductors into (3.6) and (3.7) together to get:

$$\frac{\pi^2}{2}(\frac{f_c}{f_s})^2(1-D) = \frac{\pi^2}{2}\left(\frac{1}{\frac{2\pi\times220\times10^{-6}}{200\times10^3}}\right)(1-0.5) \le 5\% \tag{8}$$

In summary, the single-ended forward power converter's isolation transformer primary winding, secondary winding and magnetic reset winding coil turns ratio is $\mathrm{N_1}$: $\mathrm{N_2}$: $\mathrm{N_3}$ = 2: 1: 2. The inductance value of the filter on the output side is 220μH, and the capacitance value is 220uF.

B. TRANSIENT ANALYSIS OF THE SWITCHING VOLTAGE

Due to the influence of parasitic inductance, parasitic capacitance and freewheeling diode, etc., undesirable overshoot and oscillation appear in the MOSFET switching process, which are the main factors that increase the electromagnetic interference. Therefore, replacing the switching transients with high overshoot and high rate of change with optimized and smooth switching waveforms can effectively suppress the electromagnetic interference generated by MOSFET high-speed switching. Considering that the hard switching waveform transient takes a certain amount of time, the switching transient can be approximated as a trapezoidal wave. Smooth the local waveforms that are prone to overshoot and oscillation in the actual switching waveform to eliminate the generation of electromagnetic interference. According to the characteristics of the convolution operation of the complex variable function: For the functions F and G, if G is a smooth function and F is a integrable function in a certain domain, the convolution F ∗ G is also a smooth function. For any integrable function F, we can simply construct a smooth function sequence Fs to approximate F. In order to facilitate modeling and simplify analysis, it is assumed that the turn-on transient waveform of the target switch waveform and the turn-off transient are axisymmetric. The switching waveform function sw(t), smoothing transient function r(t), normalized derivative function g (t), and square wave function sq (t) are assumed respectively. The voltage transient equation is [17]:

$$sw(t)=\int_{-\infty}^{+\infty} sq(\tau)\cdot g(t-\tau)d\tau=\int_{-\infty}^{+\infty} sq(t-\tau)\cdot g(\tau)d\tau \tag{9}$$

The Fourier transform of the equation (3.9) shows the frequency domain expression:

$$F_{sw}(f)=F_{sq}(f)\cdot G(f) \tag{10}$$

In Equation 10, $F_{sw}(f), F_{sq}(f)$ and $G(f)$ represent the Fourier transform expressions of $sw(t)$, $sq(t)$ and $g(t)$, respectively.

The superposition of a series of sine waves can be used to represent a simple rectangular wave and the n Fourier series coefficient expression is as follows:

$$F_{sq}(n)=A(t_0/T)\frac{\sin(n\pi f_0 t_0)}{n\pi f_0 t_0}=A(t_0/T)\sin c(n\pi f_0 t_0) \tag{11}$$

where n is the harmonic order, T is the period of the rectangular wave, f_0 is the switching frequency of the rectangular wave, and t_0 is the high-level duration of the rectangular wave. When the harmonic frequency is lower than the turn-on frequency $f_0/(\pi D)$, the slope of the low-band envelope is 0. Meanwhile, the amplitude envelope of the frequency band and the high-band falls at a slope of 20dB /dec when the harmonic frequency is higher than the turning frequency.

In the process of SiC MOSFET hard switching, considering the existence of the switching time interval, the switching transient is approximately trapezoidal. According to equations (3.10) and (3.11), the coefficient expression of Fourier series can be obtained [17] [20]:

$$F_{sw}(n)=A(t_0/T)\cdot\frac{\sin(n\pi f_0 t_0)}{n\pi f_0 t_0}\cdot\frac{\sin(n\pi f_0 \tau)}{n\pi f_0 \tau} \tag{12}$$

It can be seen from the above formula that the two corner frequencies of the spectrum envelope are $f_{c1}=1/\pi t_0$ and $f_{c2}=1/\pi\tau$ respectively. When the harmonic frequency is less than the corner frequency f_{c1}, the slope of the spectrum envelope of this switching waveform is 0, and when the harmonic frequency is greater than the corner frequency f_{c1} and less than f_{c2}, the spectrum envelope decreases with a slope of 20dB/dec. Finally, when the harmonic frequency is greater than the corner frequency f_{c2}, the spectral envelope of the switching waveform decreases with a slope of 40 dB / dec.

The rectangular wave can be regarded as a zero-order derivative, and the trapezoidal wave can be regarded as a second-order derivative. Generalized to the general case, assuming that the switch function is k-derivable and sw (k) (t) contains a total of P non-derivable points, the derivation of sw (k) (t) is as follows:

$$sw^{(k+1)}(t)=\sum_{i}^{p}A_i\delta(t-\tau_i) \tag{13}$$

where Ai is the amplitude of the ith pulse function and is the time of the ith pulse function. According to the Fourier transform of Equation 3-1, the frequency domain expression of the nth harmonic of $sw\,(t)$ is:

$$F_{sw}(n)=\frac{\sum_{i=1}^{p}Aie^{-jn2\pi f_0\tau_i}}{T(jn2\pi f_0)^{k+1}} \tag{14}$$

It can be seen from the above formula that the switching frequency, the derivative number of the waveform function, and the amplitude of the impulse signal all have a significant effect on the amplitude of the spectrum.

From (14), the uniform expression of the amplitude envelope of the high-frequency band of the switching waveform can be obtained:

$$V=20\lg\sum_{i=1}^{p}|A_i|+20\lg f_0-20(k+1)\lg(n2\pi f_0)+120 \tag{15}$$

The partial derivative of the variable n can be obtained in equation (15):

$$\frac{\partial V}{\partial n}=-20(k+1) \tag{16}$$

When the switch transient function is zero-order derivable, its high-frequency envelope decreases at a rate of −20dB/dec, and when the switch transient function is derivable at a time, its band envelope decreases at a rate of −40dB/dec. When the switch transient function is secondarily derivable, the falling speed of the envelope of the high frequency band is −60dB/dec. For two switching transient functions with the same derivative of the transient function but different frequencies, we can see from formula 3.15 that the difference

in the amplitude of the two spectra at the same frequency is:

$$\Delta V = 20\lg(1 + \frac{\Delta f_0}{f_0}) \tag{17}$$

Through the above analysis, we can see that there are many factors that affect the spectrum envelope, including the duty cycle, the derivative of the switching transient function, the switching frequency, and the switching transient time. However, in practical applications, the duty cycle and switching frequency are often fixed by engineering requirements. The conductivity of the switching transient function and the switching transient time can be set by the active voltage method. The infinitely derivable Gaussian function [19], used as a reference signal to control the switching transient is an ideal choice, and its expression is as follows:

$$g(x) = \frac{1}{\sigma_t\sqrt{2\pi}} e^{-\frac{t^2}{2\sigma_t^2}} \tag{18}$$

σ_t is a quarter of the switching transient duration τ, and the equation (18) is convolved with the rectangular wave to obtain an infinitely derivative time domain expression of the switching waveform. The spectral envelope of the Gaussian function in the high frequency band will be lower than that of the zero-order derivable and first-order derivable transient functions, so the best high-frequency noise suppression effect can be obtained. Do Fourier transform on equation 18 to get its frequency domain expression and bring it into 10 with Equation 11 to get the frequency domain expression of the infinitely derivable switching transient function:

$$F_{sw}(f) = F_{sq}(f) \cdot e^{-\tau^2(2\pi f)^2/16} \tag{19}$$

In the above formula, τ is the transient duration of the switching waveform, which is the main factor affecting the speed of the decline of the waveform spectrum. It can be clearly seen that the amplitude of the middle and high frequency band of the waveform spectrum decreases with the exponential rate. However, the reference waveform used in this article is different from the reference waveform in [19], but only the transient band of the rising and falling edges in Equation 3.19 are selected. The intermediate band of reference waveform will be designed based on the switching waveform characteristics of the single-ended forward power converter.

FIGURE 3 shows the reference signal used of the proposed method and its expression is as follows:

$$sw(t) = \begin{cases} 0 & t < 0 \\ \frac{A}{B} sq(t) * g(t) & 0 < t < t_r \\ \frac{A}{B} & t_r < t < t_1 + t_r \\ \frac{\alpha A}{B} & t_1 + t_r < t < t_2 + t_1 + t_r \\ \frac{\alpha A}{B} sq(t) * g(t) & t_2 + t_1 + t_r < t < t_2 + t_1 + t_r + t_f \\ 0 & t_2 + t_1 + t_r + t_f < t \end{cases} \tag{20}$$

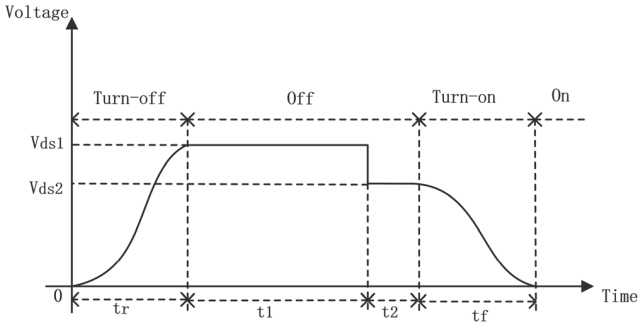

FIGURE 3. The designed Guassian reference signal for Closed-Loop Gate Drive.

where B is the value of sq (t) ∗ g (t) obtained at the time of tr, that is, the maximum value of the convolution in the interval of [0 tr], A is the amplitude of sw (t), Vds1 = A / B, α is the correction factor to deal with the phenomenon of the drop of the drain-source voltage during the off period, $\alpha A/B = V_{ds2}$. The t_r is the rise time of the reference function, which is the transient time when the SiC MOSFET is turned off, and the Gaussian signal is selected as the rising edge reference signal. Similarly t_f is the fall time of the reference signal, which is the turn-on transient time of the SiC MOSFET and the Gaussian signal as the turn-on reference signal. The time t_r and t_f can be adjusted dynamically and is an important time period that mainly determines the switching duration and switching loss, but in this article, in order to simplify the analysis, let $t_r = t_f$.

For the Gaussian signal, it takes infinite time to rise from 0 to the maximum value and to fall from the maximum value to 0, but in actual engineering, it is impossible to set a reference for a poor time, so it can only be artificially pulled down after a certain time to 0 or higher than 0. t_1 is the time when the transformer gradually releases magnetic energy from the saturation state until the magnetic flux gradually decreases to zero. t_2 is the holding time when the transformer magnetic flux is zero. It is worth mentioning that in order to quickly turn off the SiC MOSFET, V_{ds1} is usually higher than the feedback of the supply voltage V_s.

IV. SIMULATION AND ANALYSIS OF SING-ENDED FORWARD CONVERTER

A. SIMULATION ANALYSIS OF HARD SWITCHING

According to the relevant parameters calculated in Section A of III and the topology of the single-ended forward circuit, the circuit is simulated using Pspice software. The SiC MOSFET used in the simulation circuit is SCT2160KE, and SiC diode produced by ROHM It is produced by STMicroelectronics, and their models are downloaded from their official website. Its equivalent circuit is shown in FIGURE 2. The power supply Vs is a DC power supply 100V. The switch S is SCT2160KE and its drive signal frequency is 200 KHz, and the duty cycle is 0.5. The simulation results are as follows:

FIGURE 4 shows the drain-source voltage and drain current of SiC MOSFET in one cycle 5μs. In order to facilitate

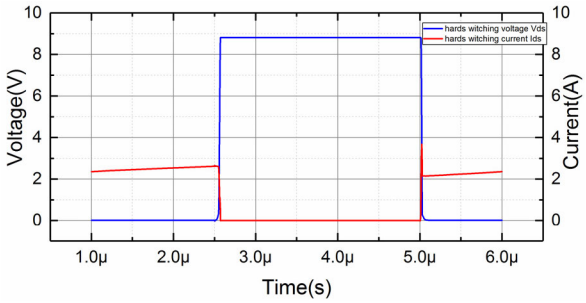

FIGURE 4. Drain-source voltage Vds and drain current Ids with hard switching control.

the display, the 200V drain-source voltage is reduced to 0.04375 times, but the drain-source current value in the figure is the real value, and the energy consumed in a cycle is about 1e-05j.

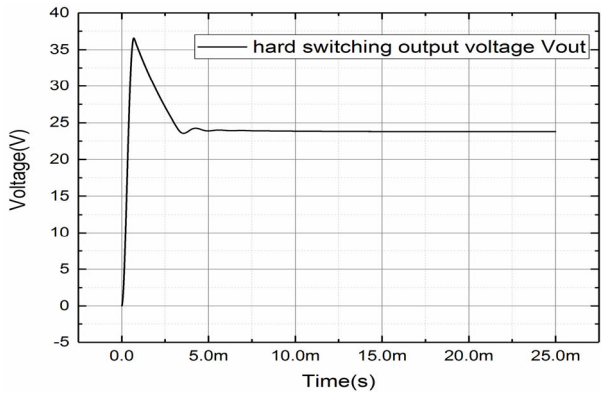

FIGURE 5. Output voltage of single-ended forward converter with hard switching control.

FIGURE 5 shows the output voltage at both ends of the load. In the FIGURE 5, the output voltage no longer fluctuates much when the circuit is turned on for approximately 10ms, and the circuit output voltage tends to stabilize. The reason why the expected value of the output voltage is 25V, but the actual value obtained by the simulation is 24.37V is that the diode conduction voltage drop and the voltage drop on the output filter inductor exist, so the simulated value should be slightly lower than the theoretical value. The voltage ripple of the converter output voltage stable part is about 0.01V, and the ripple rate is less than 5%, which meets the design requirements.

B. SIMULATION ANALYSIS OF CLOSED-LOOP GATE DRIVE CONTROL METHOD

Because the Gaussian signal has infinite conductivity, its transient waveform in the time domain is nonlinear, so closed-loop gate drive is used to compensate the nonlinearity of the switching device through the feedback loop.

The working principle of MOSFET is that when the gate voltage increases, the MOSFET tends to turn on, then the equivalent on-state resistance decreases, and the drain voltage decreases. Conversely, when the gate drive voltage decreases, MOSFET tends to turn off, then the equivalent on-state resistance increases, and the drain-source voltage increases. The basic idea of closed-loop gate drive is to introduce negative feedback in the process of MOSFET driving, which collects the switching waveform of the MOSFET through the voltage divider, then compare it with the driving reference waveform, and drive the MOS tube through the gate resistance. Then control the switch voltage of MOSFET to follow the set reference voltage waveform during operation.

The closed-loop gate circuit is shown in FIGURE 1. The reference voltage generator is used to generate the Gaussian reference waveform that has frequency 200 kHz and duty 0.5. The reference voltage generator is used to generate a Gaussian reference waveform and the high level is set to 8.75V and the low level is set to −1.25V. Both the rising and falling edge durations are set to 1 μs, and the switching frequency is set to 200 kHz, and the duty cycle is 0.5. High-bandwidth operational amplifier THS3091 produced by Texas Instruments was selected, and its Pspice simulation model was obtained from its official website. The simulation results of the closed-loop gate drive are shown in FIGURE 6 and FIGURE 7. In FIGURE 6, the results of the MOSFET drain-source feedback voltage waveform following the Gaussian reference voltage waveform are compared and it can be clearly seen that the MOSFET drain-source voltage can follow the reference waveform well so that the proposed method is feasible. It is worth mentioning that in order to ensure that the MOSFET is fully turned on, a negative voltage is set in the reference waveform which results in the drain voltage always staying at zero during the period from negative to zero. As a result, the actual switching transient time of the switching waveform is less than the switching transient time of the reference waveform.

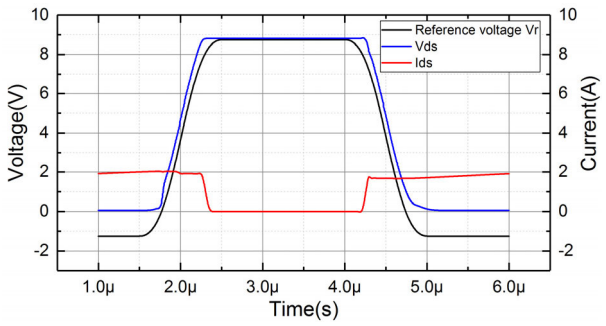

FIGURE 6. The simulation results of Drain-source voltage Vds and drain-source current Ids by closed-loop gate drive.

Gaussian waveforms with the drain-source voltage waveform amplitude 200V, a switching frequency 200 kHz, a switching time 0.5 μs, and a duty cycle 0.5 are obtained through measurement. The drain-source voltage shown in FIGURE 6 is the partial voltage of the true drain-source voltage, which is about 0.04375 times the true drain-source voltage. FIGURE 7 is the output voltage of the circuit converter at both ends of the load. After the circuit is turned

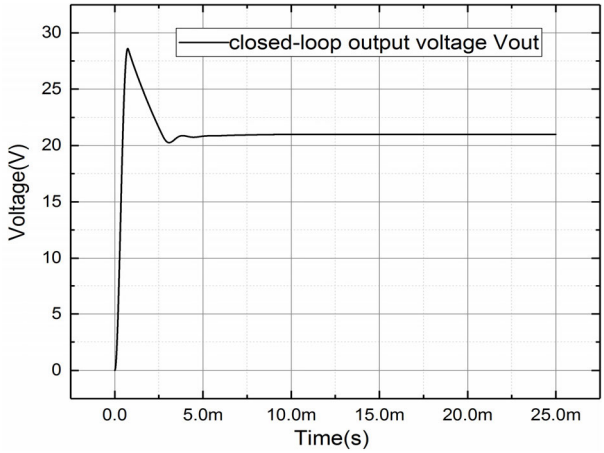

FIGURE 7. Output voltage of single-ended forward converter by hard switching control.

on for nearly 8*ms*, the output voltage no longer fluctuates greatly, and the circuit output voltage tends to be stable. The reason why the expected value of the output voltage is 25V, but the actual value obtained by simulation is 22V is that there are conduction voltage drop across the diode and the output filter inductor, and the output voltage waveform of the rectifier diode D1 is not a strict square wave and its rising and falling edges last longer, so that the equivalent average Slightly reduced and the simulated value is slightly lower than the output value under the control of the hard switch. Taking the measurement of the converter output voltage stabilization part and measuring it, the output voltage ripple is 0.01V and the ripple rate is less than 5%, which meets the design requirements. The power consumption of MOS in one cycle is 2.27e-4j with the closed-loop gate drive method.

C. ANALYSIS OF ELECTROMAGNETIC INTERFERENCE SUPPRESSION

Select the stable voltage of the single-ended forward power converter under traditional hard switching control and closed-loop gate drive control, and analyze the frequency spectrum.

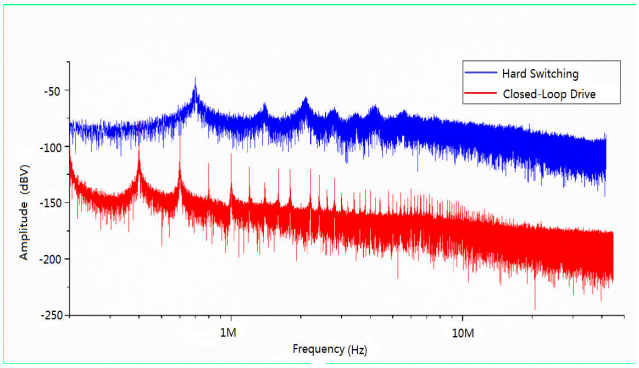

FIGURE 8. Comparison of output voltage spectrum between hard-switch control and closed-loop gate drive control.

The red frequency spectrum in FIGURE 8 is the output voltage spectrum of the closed-loop gate drive control, and the blue frequency spectrum is the output voltage spectrum of the hard switching control. The red spectrum in FIGURE 8 is the output voltage spectrum of the closed-loop gate drive control, and the blue spectrum is the output voltage spectrum of the hard switch control. The frequency band analyzed ranges from the converter switching frequency of 200 kHz to the upper limit of electromagnetic conduction interference of 30 MKHz.

Comparing the envelope of the output voltage spectrum of the two control methods, we can see: From 200 KHz to 600 KHz relatively low frequency band, the output spectrum of closed-loop gate drive control and hard switch control are not significantly different; In the relatively mid-frequency band of 600 KHz to 10 MHz, the output voltage spectrum produces 45dB attenuation compared to the hard switching method. In the relatively high frequency band of 10 MHz to 30MHz, the output voltage spectrum produces 70dB attenuation compared to the hard switching method. In general, the closed-loop gate drive control method can make the switching waveform of the MOSFET follow the reference Gaussian waveform well, which can effectively suppress the high-frequency electromagnetic interference noise of the power supply. And the electromagnetic interference suppression effect is obvious as the harmonic frequency increases.

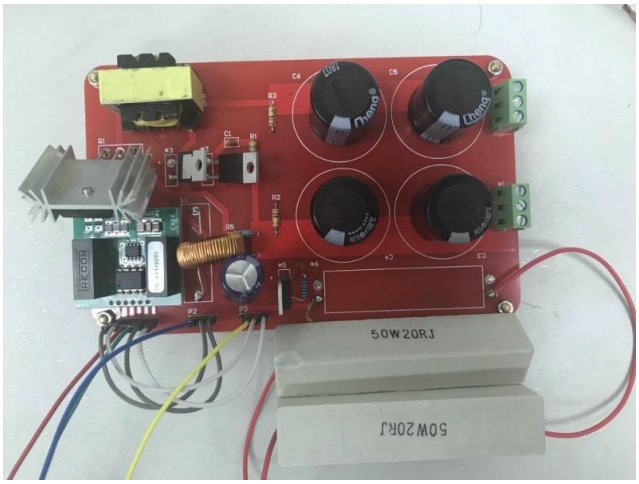

FIGURE 9. Single-ended forward circuit with hard switching.

V. EXPERIMENT AND ANALYSIS

A. SINGLE-ENDED FORWARD CIRCUIT EXPERIMENT WITH HARD SWITCHING CONTROL

FIGURE 9 shows a single-ended forward power converter controlled by hard switching. This circuit uses the traditional PWM wave as the MOSFET drive shape and this experiment aims to obtain the output voltage spectrum of the hard converter controlled by hard switching under stable operation.

This circuit mainly adopts single-ended forward circuit topology and the PWM driving waveform required for hard switch control is generated by an arbitrary waveform generator that the instrument model is AFG3021C. To avoid that the waveform generator is insufficient to drive the MOSFET,

a CRD-001 MOSFET gate driver chip produced by Cree was added between the MOSFET and the arbitrary waveform generator to increase the drive capability of the PWM wave. Due to the insufficient workmanship of the three-winding high-frequency transformer used in the experiment, the experiment showed that when the PWM wave with a duty ratio of 0.5 was used, the demagnetization winding of the transformer could not completely release the magnetic energy in the core during the MOSFET off period and then, after a certain period, the transformer saturation cannot work normally. After many adjustments, it is determined that the PWM wave with a duty ratio of 0.3 is used to drive the MOSFET. Under such conditions, within one working cycle, the demagnetization winding can just completely release the energy stored in the magnetic core and then after several duty cycle, the theoretical voltage at the load end of the circuit should be 15V but considering the conduction voltage drop of the rectifier diode and the voltage division of the filter inductor, the actual output should be slightly lower than 15V. The results of the experiment are shown in Figure10, Figure11, Figure12 and Figure13.

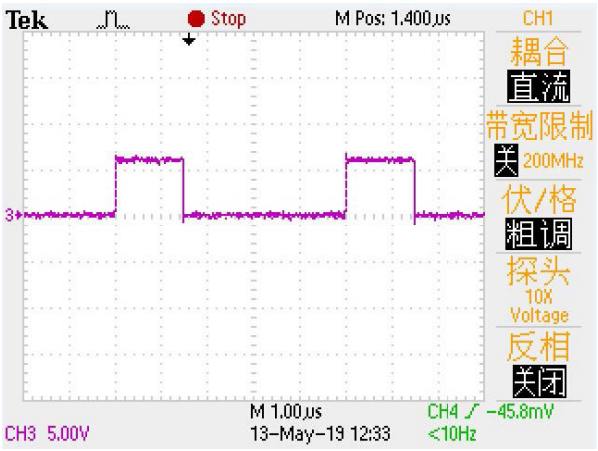

FIGURE 10. PWM of hard switching control.

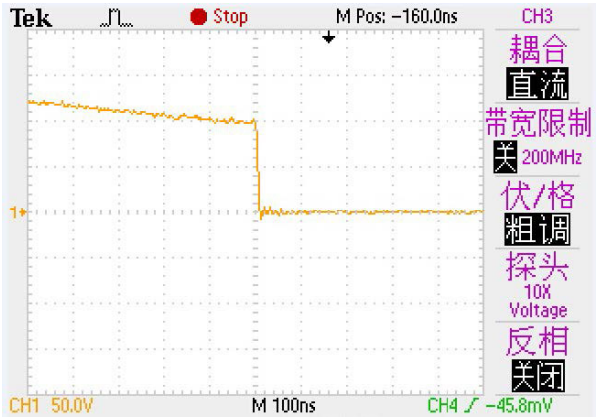

FIGURE 11. Drain-source voltage of hard switching control.

FIGURE 10 shows a PWM with a duty cycle of 0.3, a high level of 6V, a low level of 0, and a period of 8μs. FIGURE 11 shows the locally amplified voltage waveform

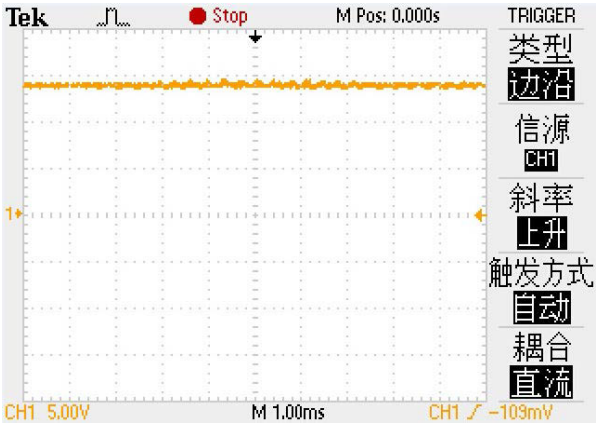

FIGURE 12. Output voltage of hard switching control.

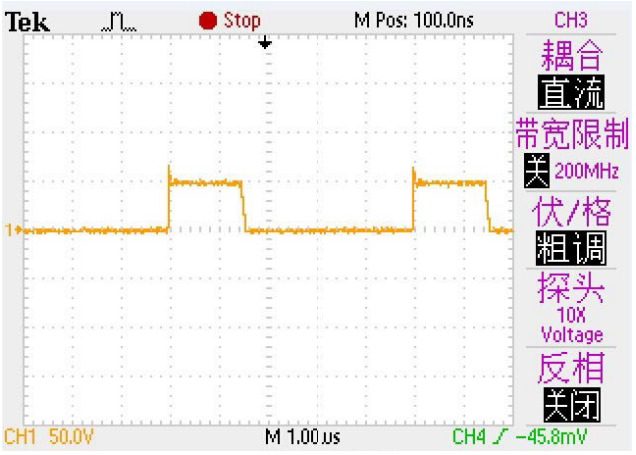

FIGURE 13. Terminal voltage of rectifier diode D1.

of the drain-source voltage of the MOSFET during the MOSFET off time and it can be seen from the figure that when the drain-source voltage drops to 100V and lasts for a very short period of time (about 100ns), the demagnetization winding can release the energy in the core completely just at the end of the cycle. FIGURE 12 shows the voltage waveform when the output of the single-ended forward circuit is stable, and the output voltage value is 14V. FIGURE 13 shows the output voltage of the rectifier diode D1 with the high level 48V, the low level 0V, the period 5μs, and the duty cycle 0.3.

B. MULTIPART FIGURES THE EXPERIMENT OF CLOSED-LOOP GATE DRIVE

Connect the closed-loop gate drive circuit to the forward power circuit to obtain a closed-loop controlled forward circuit. Set the reference Gaussian waveform duty cycle to 0.3 and the period to 5μs. The measurement results are as follows:

FIGURE 14 shows the closed-loop gate drive control circuit. The comparison between the Gaussian reference waveform and the drain-source voltage waveform of the MOSFET shows that the drain-source voltage waveform can follow

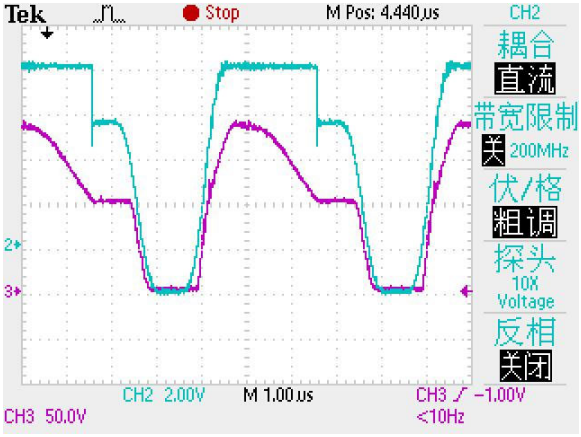

FIGURE 14. Comparison of drain-source voltage and reference Gaussian waveform with closed-loop gate drive.

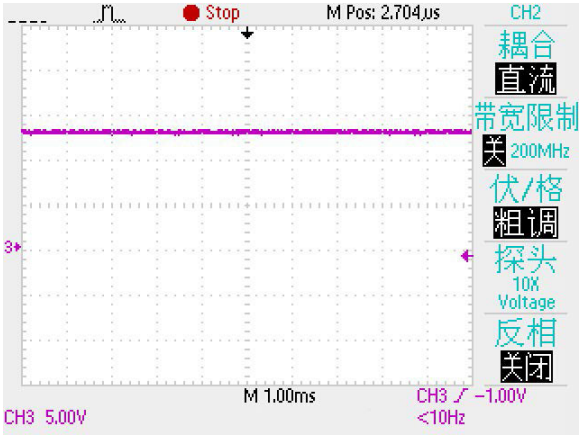

FIGURE 15. Output voltage with closed-loop grid driving method.

the reference waveform well. FIGURE 15 shows the stable waveform of the output voltage of the single-ended forward circuit with closed-loop gate drive control circuit, and the output voltage value is about 13V. The output voltage spectrum comparison between hard switching and closed-loop drive control method is as follows:

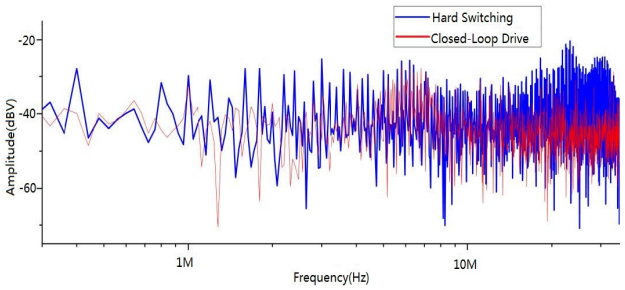

FIGURE 16. Output voltage spectrum comparison between hard switching method and closed-loop gate driving method.

The red spectrum in FIGURE 16 is the output voltage spectrum of the closed-loop gate drive experiment, and the blue spectrum is the output voltage spectrum of the hard-switch experiment. The frequency band for comparative analysis is from the transformer switching frequency of 200 kHz to the electromagnetic interference upper limit frequency of 30 MHz. Comparing the envelope of the output voltage spectrum of the two control methods: from 200 kHz to 2 MHz, the output voltage spectrum obtained by closed-loop control and hard-switch control is not significantly different; In the relative mid-band of 2 MHz to 6 MHz, the output voltage spectrum of closed-loop control method has 10 dB attenuation compared with hard-switching control method. In the relatively high frequency band of 10 MHz to 30 MHz, the output voltage spectrum of closed-loop control produces a drop of approximately 25dB compared to the output voltage spectrum of hard-switch control.

VI. CONCLUSION

In this paper, according to the voltage converter index requirements, the component parameters required for the single-ended forward power converter are calculated. Combined with the principle of the negative correlation between the gate drive voltage of the MOSFET and the equivalent on-resistance of the drain-source, and applying the principle of differential amplification, the closed-loop gate drive circuit of the MOSFET is designed. The Gaussian reference signal is designed based on the relationship between the derivative order of the transient function and the spectrum envelope and the output voltage characteristics as constraints. Both simulation and experimental results show that the output voltage obtained by the closed-loop gate drive method has a significant attenuation of the electromagnetic interference compared with the traditional hard switching method in relatively medium and high frequency bands and the electromagnetic interference suppression effect is more significant with the increase of harmonic frequency. It proves that in the single-ended forward conversion circuit, the closed-loop gate drive method is effective in suppressing conducted electromagnetic interference by shaping the switching waveform. It is worth mentioning that, under the condition of setting related parameters, the switching loss of the closed-loop gate driving method is 2.27e-4j, which is 22.7 times higher than that of the hard switching method of 1e-05j. The reason is that the switch transient time of the proposed method is longer compared with the hard switching method. However, by selecting a high-frequency operational amplifier, the reference signal switching transient time can be reduced to further reduce the switching loss of the closed-loop gate driving method.

REFERENCES

[1] B. R. Lin and H. Y. Shih, "Implementation of a parallel zero-voltage switching forward converter with less power switches," *IET Power Electron.*, vol. 4, no. 2, pp. 248–256, Feb. 2011.

[2] A. Abramovitz, T. Cheng, and K. Smedley, "Analysis and design of forward converter with energy regenerative snubber," *IEEE Trans. Power Electron.*, vol. 25, no. 3, pp. 667–676, Mar. 2010.

[3] J. Jiraprasertwong and C. Jettanasen, "Analysis and mitigation of conducted electromagnetic interference in a photovoltaic single-phase inverter," in *Proc. IEEE Region 10 Conf. (TENCON)*, Bangkok, Thailand, Oct. 2014, pp. 1–5.

[4] D. Hamza, M. Sawan, and P. K. Jain, "Suppression of common-mode input electromagnetic interference noise in DC-DC converters using the active filtering method," *IET Power Electron.*, vol. 4, no. 7, pp. 776–784, 2011.

[5] M. R. Yazdani and H. Farzanehfard, "Conducted electromagnetic interference analysis and mitigation using zero-current transition soft switching and spread spectrum techniques," *IET Power Electron.*, vol. 5, no. 7, pp. 1034–1041, Aug. 2012.

[6] *Information Technology Equipment-Radio Disturbance Characteristics-Limits and Methods of Measurement-Publication 22*, CISPR, IEC Int. Special Committee Radio Interference, Geneva, Switzerland, 1997.

[7] *Limits and Methods of Measurement of Radio Disturbance Characteristics of Industrial, Scientific and Medical (ISM) Radio-Frequency Equipment*, Standard BS EN 55011, 1997.

[8] T. Guo, D. Y. Chen, and F. C. Lee, "Separation of the common-mode- and differential-mode-conducted EMI noise," *IEEE Trans. Power Electron.*, vol. 11, no. 3, pp. 480–488, May 1996.

[9] C. D. Bridge, "Clamp voltage analysis for RCD forward converters," in *Proc. 15th Annu. IEEE Appl. Power Electron. Conf. Expo. (APEC)*, vol. 2, New Orleans, LA, USA, Feb. 2000, pp. 959–965.

[10] A. Çoban and I. Çadirci, "Active clamped two-switch forward converter with a soft switched synchronous rectifier," *IET Power Electron*, vol. 4, no. 8, pp. 908–918, Sep. 2011.

[11] M. R. Yazdani, J. Faiz, and N. Amini Filabadi, "Conducted electromagnetic interference evaluation of forward converter with symmetric topology and passive filter," *IET Power Electron.*, vol. 7, no. 5, pp. 1113–1120, May 2014.

[12] B.-R. Lin and J.-J. Chen, "Analysis of an integrated flyback and zeta converter with active clamping technique," *IET Power Electron.*, vol. 2, no. 4, pp. 355–363, Jul. 2009.

[13] F. Chen, A. Amirahmadi, and I. Batarseh, "Zero voltage switching forward-flyback converter with efficient active LC snubber circuit," in *Proc. IEEE Appl. Power Electron. Conf. Expo. (APEC)*, Fort Worth, TX, USA, Mar. 2014, pp. 2041–2047.

[14] N. Boonpirom, "Conducted and radiated noise reduction using circuit balance on double switch converter," in *Proc. Conf. IPEC*, Singapore, Oct. 2010, pp. 317–322.

[15] M. R. Yazdani and A. Ariyan, "EMI reduction of a soft-switched high step-down converter using passive compensation method," in *Proc. Int. Conf. Appl. Electron. (AE)*, Pilsen, Czech Republic, Sep. 2018, pp. 1–6.

[16] N. Sudhakar, N. Rajasekar, and A. S. Shanmuga, "FPGA based chaotic PWM combined with soft switching for effective EMI mitigation in boost converter," in *Proc. Int. Conf. Energy Efficient Technol. Sustainability (ICEETS)*, Apr. 2016, pp. 148–152.

[17] F. Costa and D. Magnon, "Graphical analysis of the spectra of EMI sources in power electronics," *IEEE Trans. Power Electron.*, vol. 20, no. 6, pp. 1491–1498, Nov. 2005.

[18] P. R. Palmer and H. S. Rajamani, "Active voltage control of IGBTs for high power applications," *IEEE Trans. Power Electron.*, vol. 19, no. 4, pp. 894–901, Jul. 2004.

[19] X. Yang, Y. Yuan, X. Zhang, and P. R. Palmer, "Shaping high-power IGBT switching transitions by active voltage control for reduced EMI generation," *IEEE Trans. Ind. Appl.*, vol. 51, no. 2, pp. 1669–1677, Mar. 2015.

[20] T. Cui, Q. Ma, P. Xu, and Y. Wang, "Analysis and optimization of power MOSFETs shaped switching transients for reduced EMI generation," *IEEE Access*, vol. 5, pp. 20440–20448, 2017.

[21] M. R. Yazdani, N. Amini Filabadi, and J. Faiz, "EMI examination of symmetric forward converter," in *Proc. 4th Annu. Int. Power Electron., Drive Syst. Technol. Conf.*, Tehran, Iran, Feb. 2013, pp. 367–371.

[22] X. Wei, C. Luo, H. Nan, and Y. Wang, "A simple structure of zero-voltage switching (ZVS) and zero-current switching (ZCS) buck converter with coupled inductor," *J. Power Electron.*, vol. 15, no. 6, pp. 1480–1488, Nov. 2015.

[23] J. Chen, *Power Electronics*. Beijing, China: Higher Education Press (in Chinese), 2011.

CONGWEN XU was born in Shandong, China, in 1991. He received the B.Eng. degree from Shandong Normal University, Jinan, China, in 2014. He is currently pursuing the Ph.D. degree with the School of Automation Science and Electronic Engineering, Beihang University, Beijing, China. His researching interests mainly include power converter electromagnetic interference simulation and recognition and suppression.

QISHUANG MA received the Ph.D. degree in electrical engineering from Xi'an Jiaotong University, Xi'an, China, in 1994. From 1994 to 1996, he was with the Electrical Engineering Center, Huazhong University of Science and Technology, Wuhan, China, for postdoctoral studies. In 1996, he became an Assistant Professor. Since 2000, he has been a Professor with the School of Automation Science and Electrical Engineering, Beihang University, Beijing, China. His research interests include power systems, electric systems, and magnetic field.

PING XU received the Ph.D. degree in electrical engineering from Beihang University, Beijing, China, in 2012. Since 2012, she has been with the School of Automation Science and Electrical Engineering, Beihang University. Her research interests include electric systems and electromagnetic compatibility.

NAN WANG received the B.Eng. and M.Phil. degrees in electrical engineering from Beihang University, Beijing, China, in 2017 and 2020, respectively. His research interests mainly include power converter electromagnetic interference simulation and suppression.